Three-Dimensional Hydrazone-Equipped Covalent Organic Frameworks as pH-Triggered Rotary Switches

Wenjuan Zhao, Chengyang Yu, Jie Zhao, Fengqian Chen, Xinyu Guan, Hui S Li, Bin Tang, Guangtao Yu, Valentin Valtchev, Yushan Yan, et al.

Three-Dimensional Hydrazone-Equipped Covalent Organic Frameworks as pH-Triggered Rotary Switches

Wenjuan Zhao, Chengyang Yu, Fengqian Chen, Xinyu Guan, Hui Li, Bin Tang, Valentin Valtchev, Yushan Yan, Shilun Qiu, and Qianrong Fang**

W. Zhao, C. Yu, F. Chen, X. Guan, Dr. H. Li, Prof. S. Qiu, Prof. Q. Fang
State Key Laboratory of Inorganic Synthesis and Preparative Chemistry, Jilin University,Changchun 130012, China
E-mail: qrfang@jlu.edu.cn
Dr. B. Tang
Deakin University, Institute for Frontier Materials, Geelong, Victoria 3216, Australia
E-mail: bin.tang@deakin.edu.au
Prof. V. Valtchev
Qingdao Institute of Bioenergy and Bioprocess Technology, Chinese Academy of Sciences, Qingdao, Shandong 266101, China
Normandie Univ, ENSICAEN, UNICAEN, CNRS, Laboratoire Catalyse et Spectrochimie, 14050 Caen, France
Prof. Y. Yan
Department of Chemical and Biomolecular Engineering, Center for Catalytic Science and Technology, University of Delaware,Newark, DE 19716, USA

Abstract: The properties expansion of three-dimensional (3D) functionalized covalent organic frameworks (COFs) is important for developing their potential applications. Herein, we report the first case of 3D hydrazone-based COFs as pH-triggered molecular switches and explore their application in the stimuli-responsive drug delivery system. These functionalized COFs with hydrazone groups on the channel walls were obtained via a multi-component bottom-up synthesis strategy. They exhibit a good invertibility E/Z isomerization at various pH values, confirmed by UV-vis absorption spectroscopy and favorable proton conduction. Remarkably, after loading cytarabine (Ara-C) as a model drug molecule, these pH-responsive COFs showed an excellent and intelligent sustained-release effect. They showed an almost 4-fold increase in the Ara-C release at pH=4.8 than at pH=7.4, which will effectively improve drug-targeting and reduce drug side effects. Thus, these results open a way toward designing 3D stimuli-responsive functionalized COF materials and promote their potential applications as carriers in the field of disease treatment.

Keywords: covalent organic frameworks · functionalization · stimuli-responsive · drug release

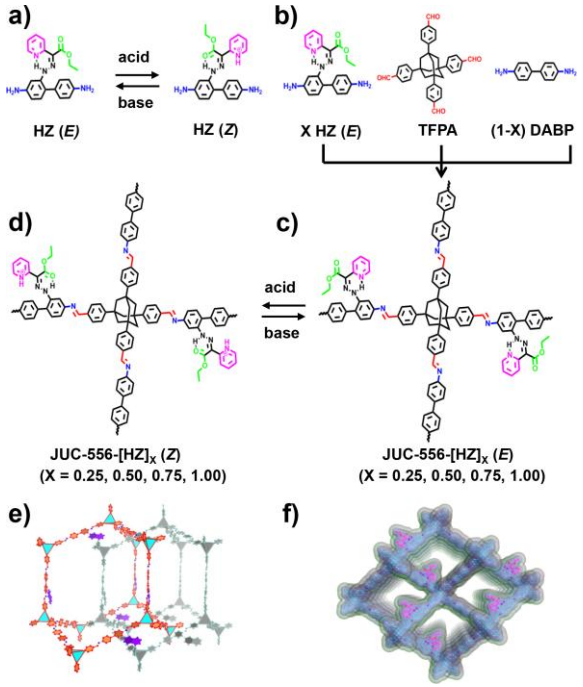

Scheme 1. Schematic representation of the strategy for preparing JUC-556-$[HZ]_X$ with *E/Z* isomerization. (a) Acid/base controlled *E/Z* isomerization of free HZ molecule. (b) Molecular structures of TFPA as a tetrahedral building unit as well as HZ (*E*) and DABP as linear linkers. (c) JUC-556-$[HZ]_X$ (*E*) constructed by the condensation reaction of TFPA with HZ (*E*) and/or DABP. (d) Acid/base controlled *E/Z* isomerization in JUC-556-$[HZ]_X$. (e) 2-fold interpenetrated **dia** network in JUC-556-$[HZ]_X$ (*E*). (f) Structural representation of JUC-556-$[HZ]_X$ (*E*).

Covalent organic frameworks (COFs) are a new class of porous crystalline polymers, which allow crystallographically precise integration of building blocks into their periodic structures. [1] The potential applications of COFS are in various fields, including gas adsorption and separation,[2] organic electronics,[3] heterogeneous catalysis,[4] and some others.[5] At present, most of the discovered COFs are still two-dimensional (2D) frameworks with eclipsed stacking structures because of their more simple synthesis and easier functionalization. Compared with 2D analogues, three-dimensional (3D) functionalized COFs have recently attracted more and more attention due to their higher specific surface areas and unique pore structures.[6] For example, through bottom-up or post-synthetic strategy, we have acquired a series of 3D functionalized COF materials,[7] e.g., 3D tetrathiafulvalene-based COFs for tunable electrical conductivity,[7a] 3D carboxy-functionalized COF for selective ion adsorption,[7b] and 3D salphen-based COFs for catalytic antioxidants.[7c] Despite significant efforts in the *in situ* synthesis and post-synthesis modifications, the functionalization of 3D COFs remains largely unexplored up to now, and especially 3D architectures with stimuli-responsive behaviors have barely been reported.

It is well-known that hydrazone and its derivatives are significant synthons for numerous transformations, and their C=N groups can undergo efficiently reversible structures between *E* and *Z* configurations in the presence of acid or base (Scheme 1a).[8 Consequently, pH-triggered hydrazone-based switches are widely incorporated into various materials,[9] including supramolecular systems, liquid crystals, and gel to achieve such unique properties. Recently, some 2D hydrazone-based COFs have been reported,[10] such as COF-42[10a] and TFPPy-DETHz-COF,[10b] in which hydrazone building units are used as the backbone of frameworks. Thus their applications as stimuli-responsive materials are greatly hindered. In principle, the combination of hydrazone-based building blocks as side chains and the interconnected channels in 3D COFs will be greatly beneficial for the preparation of stimuli-responsive materials. However, none of the hydrazones has been integrated into the 3D COF framework because of the crystallization and structural problems.

Herein, we report the synthesis of 3D hydrazone-equipped COFs and study their application as pH-triggered rotary switches in the stimuli-controlled release of a drug molecule. Different from previous reports, the hydrazone groups, in this case, were decorated on the channel walls of COFs by a multi-component bottom-up synthesis strategy. The obtained structures showed well-behaved invertibility of *E/Z* isomerization at different pH values, which was confirmed by proton conduction and UV-vis absorption analysis. More importantly, after loading drug molecule (cytarabine, Ara-C), these stimuli-responsive COFs demonstrated exceptional release effects for Ara-C with an almost 4-fold amplification at pH=4.8 than at pH=7.4. This is the first example of 3D hydrazone-functionalized COFs and their application for pH-responsive drug delivery to the best of our knowledge.

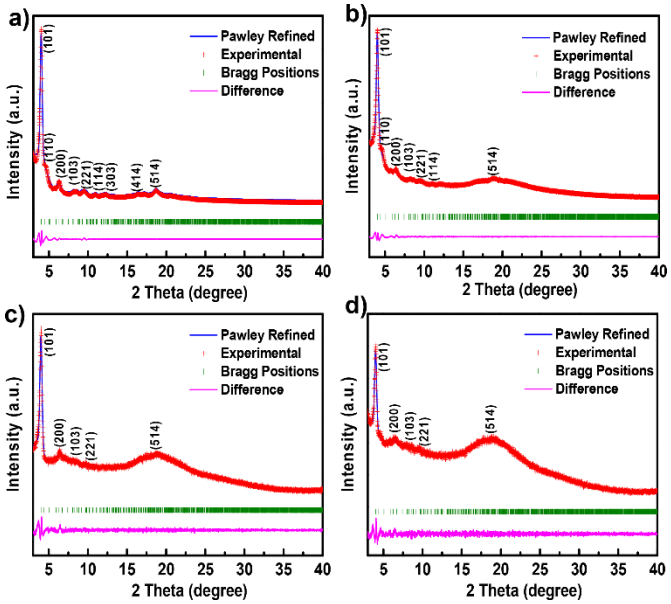

Figure 1. PXRD patterns of JUC-556-$[HZ]_{0.25}$ (*E*) (a), JUC-556-$[HZ]_{0.50}$ (*E*) (b), JUC-556-$[HZ]_{0.75}$ (*E*) (c), and JUC-556-$[HZ]_{1.00}$ (*E*) (d).

Our strategy for constructing 3D stimuli-responsive COFs is based on a hydrazone derivative with *E*/*Z* interconversion, (*E*)-ethyl-2-(2-(4,4'-diaminobiphenyl)hydrazono)-2-(pyridin-2-yl) acetate (HZ (*E*),(Scheme 1a). To maximize the functionalization of materials while maintaining their crystallinity and porosity, we have employed a multi-component condensation system to synthesize a series of 3D hydrazone-based COFs. As shown in Scheme 1b, 4,4'-diaminobiphenyl (DABP) and HZ (*E*) were chosen as linear linkers, while 1,3,5,7-tetrakis(4-formylphenyl)adamantane (TFPA) was synthesized as an ideal tetrahedral building unit. The condensation of TFPA with DABP or/and HZ (*E*) produced 3D COFs with different amounts of HZ (*E*), JUC-556-$[HZ]_X$ (*E*), where X is the proportion of functional group HZ (*E*) (X = [HZ (*E*)]/([DABP]+[HZ (*E*)]); X = 0.25, 0.50, 0.75 or 1.00; Scheme 1c). Similar to HZ (*E*) building unit, JUC-556-$[HZ]_X$ (*E*) were considered providing acid/base controlled *E/Z* isomerization (Scheme 1d). Composed from linear and tetrahedral building blocks and subjected to the large steric effect of HZ (*E*) groups, these COFs are expected to exhibit a 2-fold interpenetrated diamondoid (**dia**) network (Scheme 1 e).[11]

Typically, JUC-556-$[HZ]_X$ (*E*) were synthesized by suspending DABP and/or HZ (*E*) with TFPA in the mixed solvent of dioxane and mesitylene in the presence of acetic acid followed by heating at 120 °C for 3 days. These condensation reactions exhibited similar isolated yields (80%), indicating that the reactivities of DABP and HZ (*E*) were similar (Supporting Information, Section 1). The structural characterization of JUC-556-$[HZ]_X$ (*E*) was executed combiniiinggg complementary methods. Scanning electron microscopy (SEM) indicated that JUC-556-$[HZ]_X$ (*E*) showed rod-shaped crystals (Figures S1-4). In Fourier transform infrared (FTIR) spectra of JUC-556-$[HZ]_X$ (*E*), the peaks assigned to C=N stretching vibration appeared at about 1615 cm^{-1}, demonstrating the formation of imine linkages (Figures S5-8). The solid-state ^{13}C cross-polarization magic-angle-spinning (CP/MAS) NMR spectra further confirmed the presence of imine linkages in the light of the distinguishing C=N signals at about 152 ppm for JUC-556-$[HZ]_X$ (*E*) (Figures S9-12). According to the thermogravimetric analysis (TGA), JUC-556-$[HZ]_X$ (*E*) started to lose weight at 250 °C due to the decomposition of monomer HZ (*E*), and overall skeletons were stable up to about 500 °C in the nitrogen atmosphere (Figures S13-17). Furthermore, the crystalline structures of JUC-556-$[HZ]_X$ (*E*) can be maintained in a variety of organic solvents and aqueous solutions with a series of pH values (Figures S18-21), verifying their remarkable stability.

The crystalline structures of JUC-556-$[HZ]_X$ (*E*) were revealed by powder X-ray diffraction (PXRD) analysis (Figure 1). Herein we took JUC-556-$[HZ]_{0.25}$ (*E*) as an example to analyze their structures (Figure 1a). The unit cell parameters of JUC-556-$[HZ]_{0.25}$ (*E*) were resolved by the PXRD pattern in conjunction with structural simulation. After a geometrical energy minimization by using the Materials Studio software package[12] based on a 2-fold interpenetrated **dia** net and disordered HZ (*E*) structures,[13] the unit cell parameters of JUC-556-$[HZ]_{0.25}$ (*E*) were obtained ($a = b = 28.2591$ Å, $c = 34.7253$ Å and $\alpha = \beta = \gamma = 90°$). The simulated PXRD pattern was in good agreement with the experimental one (Figure 1a). Furthermore, the full profile pattern matching (Pawley) refinement was performed from the experimental PXRD pattern. The strong PXRD peaks at 4.03, 5.11, 6.25, 8.27, 9.20, 11.10, 12.18, 16.42, and 18.98° 2θ for JUC-556-$[HZ]_{0.25}$ (*E*) can be assigned to the (101), (110), (200), (103), (221), (114), (303), (414), and (514) Bragg peaks of a tetragonal space group $P4_2/n$ (No. 86), respectively. The refinement results revealed that unit cell parameters were nearly equivalent to the predicted ones with excellent agreement factors ($a = b = 28.3520$ Å, $c = 34.8160$ Å, $\alpha = \beta = \gamma = 90°$, $\omega Rp = 5.77\%$, and $Rp = 4.29\%$). In addition, we also examined alternative structures, such as non- or 3-fold interpenetrated **dia** network. However, there were significant differences between the simulated and experimental PXRDs (Figures S22-25). As the HZ (*E*) content increases, the crystallinity of JUC-556-$[HZ]_X$ (*E*) decreases slightly due to disordered HZ (*E*) units on the channel walls; however, these materials also exhibit similar diffraction patterns, indicating that they have the same structures (Figure 1b-d). Based on the above results, it is proposed that JUC-556-$[HZ]_X$ (*E*) have the expected architectures with a 2-fold interpenetrated **dia** net, and microporous cavities with a diameter of about 1.70 nm (Scheme 1f).

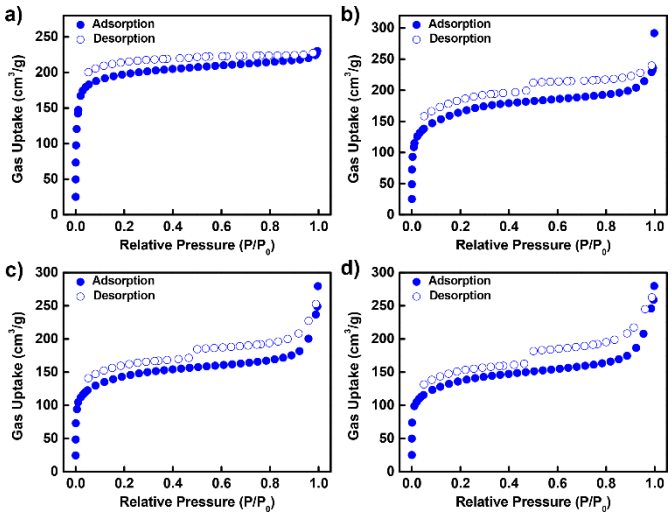

Figure 2. N_2 adsorption-desorption isotherms for JUC-556-$[HZ]_{0.25}$ (*E*) (a), JUC-556-$[HZ]_{0.50}$ (*E*) (b), JUC-556-$[HZ]_{0.75}$ (*E*) (c), and JUC-556-$[HZ]_{1.00}$ (*E*) (d) at 77 K.

The porosity and specific surface areas of JUC-556-$[HZ]_X$ (*E*) were analyzed by nitrogen gas adsorption measurements at 77 K (Figure 2). A sharp increase in gas uptake at low pressure (below 0.1 P/P_0) demonstrated the microporous nature of JUC-556-$[HZ]_X$ (*E*). An inclination of the isotherm and slight desorption hysteresis was observed, implying the presence of textural mesopores caused by the agglomeration of COF crystals.[7e] Their surface areas exhibited a decreasing tendency with the raise of HZ (*E*) content. The Brunauer-Emmett-Teller (BET) surface areas were 634 m^2/g for JUC-556-$[HZ]_{0.25}$ (*E*), 527 m^2/g for JUC-556-$[HZ]_{0.50}$ (*E*), 467 m^2/g for JUC-556-$[HZ]_{0.75}$ (*E*) and 430 m^2/g for JUC-556-$[HZ]_{1.00}$ (*E*), respectively (Figures S26-29). Based on nonlocal density functional theory (NLDFT), JUC-556-$[HZ]_X$ (*E*) showed similar microporous diameters of 1.62-1.80 nm (Figures S30-33), which were in good agreement with the pore sizes predicted from their crystal structures (1.70 nm).

Inspired by the abundant presence of HZ dangling groups, we ve studied the pH-triggered rotary switching effect of JUC-556-$[HZ]_X$ under different pH conditions (Figures 3 and S34-62). The acid/base induced *E/Z* isomerization of dissociative HZ units was first inspected by UV-vis absorption spectroscopy, and the results clearly showed that the pH-triggered switching processes was reversible (Figures S34-44). Similar to free HZ units, JUC-556-$[HZ]_X$ also exhibited good pH-responsive switching behaviors. The color of the as-synthesized JUC-556-

$[HZ]_X$ (*E*) evolved gradually from yellow to red upon acid treatment, due to the sensitive *E/Z* isomerization to various pH values (Figure S45). Furthermore, the evolution of UV-vis absorption spectra verified the *E/Z* configurational changes. JUC-556-$[HZ]_{0.50}$ (*E*) was selected as an example to illustrate the acid-base isomerization. When JUC-556-$[HZ]_{0.50}$ (*E*) was titrated with trifluoroacetic acid (TFA, Figures 4a and S46), the intensity of the absorption band at 283 nm decreased whereas that at 249 nm increased as the amount of the added acid increased. The spectral conversion clearly indicated that the HZ groups of the JUC-556-$[HZ]_{0.50}$ (*E*) underwent the configurational changes from *E* to *Z*. Upon the addition of triethylamine (Et_3N) to the sample of JUC-556-$[HZ]_{0.50}$ (*Z*) (Figure 3b and S47), the absorption band of 283 nm restored, accompanying declining and subsequently disappearing of the absorption band at 249 nm. JUC-556-$[HZ]_{0.50}$ (*E*) also showed good pH-triggered switching processes upon the addition of TFA/Et_3N with low concentrations and remarkable reversibility (Figure 4 c-e). It should be noted that the transformations of colors and UV-vis absorption spectra of JUC-556-$[HZ]_X$ were slightly different from those of free HZ, which could be caused by steric hindrance and confinement effects of COF channels as well as potential inductive effects of atoms around HZ units.[8a] Furthermore, the spectral conversion of JUC-556-$[HZ]_{0.50}$ (*E*) occurred with other acids, such as HCl (Figures 4f and S48). As for other JUC-556-$[HZ]_X$ (*E*), similar acid/base dependent changes of UV-vis absorption spectra were observed, and their *E/Z* configurations were also reversible under acidic/basic conditions (Figures S49-62).

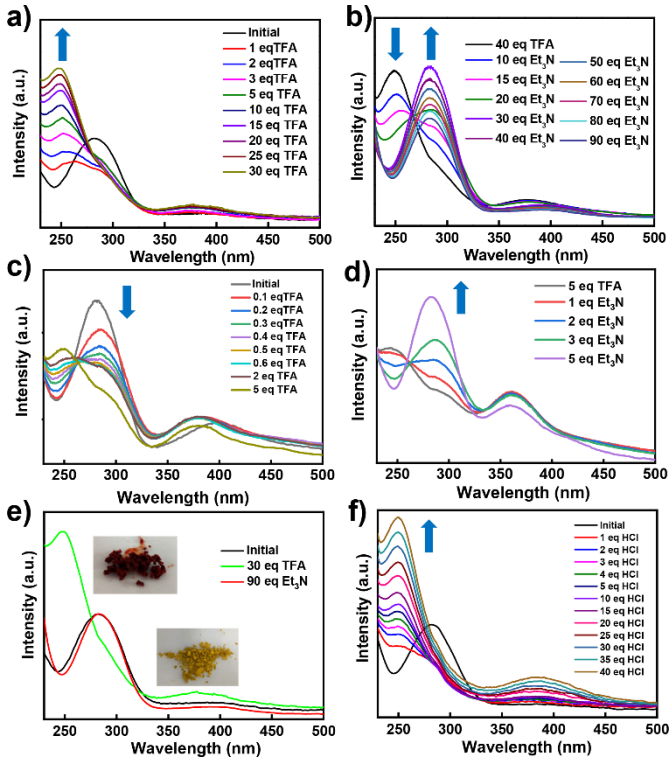

Figure 3. (a) Absorption spectra of JUC-556-$[HZ]_{0.50}$ (*E*) upon protonation in TFA solution with increasing concentrations. (b) Absorption spectra of JUC-556-$[HZ]_{0.50}$ (*Z*) upon deprotonation in Et_3N solution with increasing concentrations. (c) Absorption spectra of JUC-556-$[HZ]_{0.50}$ (*E*) upon protonation in TFA solution under low concentrations. (d) Absorption spectra of JUC-556-$[HZ]_{0.50}$ (*Z*) upon deprotonation in Et_3N solution under low concentrations. (e) Reversible change of JUC-556-$[HZ]_{0.50}$ (*E*) in the acid/base solution. Inset: the color change of JUC-556-$[HZ]_{0.50}$ (*E*). (f) Absorption spectra of JUC-556-$[HZ]_{0.50}$ (*E*) upon protonation in HCl solution with increasing concentrations.

Furthermore, the *E/Z* isomerization of JUC-556-$[HZ]_X$ was demonstrated by proton conduction at room temperature (Figures 4 and S63-66). Compared with benzene ring and imine, HZ (*E*) unit was more prone to protonation. As HZ (*E*) has rich nitrogen atoms, it can combine with HCl to form hydrogen bonds,[14] and therefore, the as-synthesized JUC-556-$[HZ]_X$ (*E*) possessed the ability to accept protons. Typically, JUC-556-$[HZ]_X$ (*E*) were compressed into cylindrical pellets with a diameter of 6.0 mm and a thickness of 1.0 mm. The proton conductivities of the original JUC-556-$[HZ]_X$ (*E*) were 2.73×10^{-6} S m^{-1} for JUC-556-$[HZ]_{0.25}$ (*E*), 3.70×10^{-7} S m^{-1} for JUC-556-$[HZ]_{0.50}$ (*E*), 1.32×10^{-6} S m^{-1} for JUC-556-$[HZ]_{0.75}$ (*E*), and 3.91×10^{-7} S m^{-1} for JUC-556-$[HZ]_{1.00}$ (*E*), respectively. Remarkably, upon protonation with HCl vapor, the proton conductivities of activated JUC-556-$[HZ]_X$ (*Z*) increased up to 4.41×10^{-4} S m^{-1} for JUC-556-$[HZ]_{0.25}$ (*Z*), 7.04×10^{-4} S m^{-1} for JUC-556-$[HZ]_{0.50}$ (*Z*), 2.17×10^{-4} S m^{-1} for JUC-556-$[HZ]_{0.75}$ (*Z*), and 3.30×10^{-4} S m^{-1} for JUC-556-$[HZ]_{1.00}$ (*Z*), which are 162-fold, 1903-fold, 164-fold, and 844-fold improvement than those of the original ones, respectively. Furthermore, the proton conductivity dropped when the JUC-556-$[HZ]_X$ (*Z*) were treated with Et_3N vapor, indicating that the pH switching process was reversible.

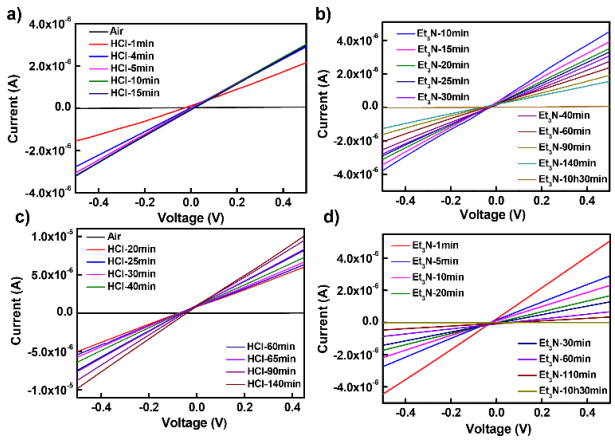

Figure 4. (a) Proton conductivity of activated JUC-556-$[HZ]_{0.25}$ (*E*) in contact with HCl vapor. (b) Proton conductivity of JUC-556-$[HZ]_{0.25}$ (*Z*) in contact with Et_3N vapor. (c) Proton conductivity of activated JUC-556-$[HZ]_{0.50}$ (*E*) in contact with HCl vapor. (d) Proton conductivity of JUC-556-$[HZ]_{0.50}$ (*Z*) in contact with Et_3N vapor.

Given the high porosity and stability of JUC-556-$[HZ]_X$ (*E*) as well as favorable pH-responsive HZ units, we explored their potential application in the stimuli-responsive drug delivery system. Ara-C, with a molecular size of about 0.9 nm was chosen as a model molecule because it is a traditional drug for cancer therapy, especially for pancreatic cancer, acute myelogenous leukemia and chronic lymphoma.[15] Typically, the JUC-556-$[HZ]_X$ (*E*) were immersed in Ara-C aqueous solution for 9 h under stirring at 200 rpm, and Ara-C-loaded JUC-556-$[HZ]_X$ (*E*) were confirmed by UV-vis absorption spectra (Figure S67). Then, the mixtures were filtered and washed. The resultant PXRD peaks coincided with those of starting materials, confirming the structural integrity after loading Ara-C (Figures S68-71). Each Ara-C-loaded JUC-556-$[HZ]_X$ (*E*) was transferred to two ampoules containing 5.0 mL releasing medium separately, and the maximum UV-vis absorption intensity at 272 nm was chosen to indicate the drug concentration during the drug-releasing process. It is known that the cancer tissues generally exist in acidic extracellular environments with pH 4 to 6. Therefore, we chose acetic acid buffer with pH 4.8 as simulated cancer fluid to release the drug. The pH in the normal physiological environment is almost neutral. Therefore, a phosphate buffer (pH = 7.4) was used to simulate normal body fluid.[16] All JUC-556-$[HZ]_X$ showed smart drug sustained-release effects in two buffer solutions (Figures 5b and S72-74). Among them, JUC-556-$[HZ]_{0.50}$ displayed the best performance in the release of drug, and the release rate reached 74.56% in the pH = 4.8 buffer within 72 h (*Z* isomerization), but only 18.59% in the pH = 7.4 buffer (*E* isomerization, Figure 5b). The release rate of drug molecule under acidic conditions was nearly 4-fold higher than that under neutral conditions, greatly improving the drug targeting delivery and reducing its side effects. Furthermore, JUC-556-$[HZ]_{0.50}$ with *E* or *Z* isomerization exhibited reproduced identical effect for the capture and release of Ara-C even after 5 cycles (Figure 5c).

As for the drug release mechanism, it is suggested that the HZ unit as a pH-responsive rotary switch in JUC-556-$[HZ]_X$ plays a key role, which can form a variety of hydrogen bonds with drug molecules.[17] When the solution is neutral or basic, the hydrogen bonds between Ara-C and HZ (*E*) units promote the loading of Ara-C onto JUC-556-$[HZ]_X$ (*E*). Meanwhile, the channels of JUC-556-$[HZ]_X$ (*E*) provide the platforms for encapsulating Ara-C. On the contrary, when the surrounding was acidic, JUC-556-$[HZ]_X$ (*E*) transforms to *Z*-type configuration through the protonation of pyridine subunits, and simultaneously Ara-C was also protonated. The repulsion between JUC-556-$[HZ]_X$ (*Z*) and Ara-C can drive the high-efficiency release of Ara-C at the acidic condition (Figure 5a).

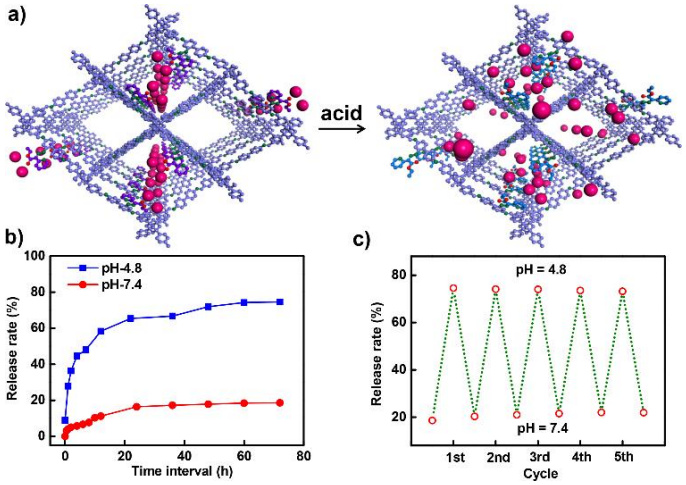

Figure 5. (a) Schematic representation of the release of Ara-C from the channels of JUC-556-$[HZ]_{0.50}$ (*Z*) in acidic solution. Drug release profiles (b) and reversibility (c) of Ara-C-loaded JUC-556-$[HZ]_{0.50}$ in simulated cancer fluid (pH = 4.8 buffer solution) and in simulated normal body fluid (pH = 7.4 buffer solution).

In conclusion, we have synthesized a series of novel 3D hydrazone-based COFs, JUC-556-$[HZ]_X$ (*E*), as pH-triggered rotary switches via the bottom-up and multi-component approach. JUC-556-$[HZ]_X$ (*E*) showed high crystallinity, good chemical stability, and reversible *E/Z*

isomerization at various pH values verified by UV-vis absorption spectroscopy and proton conduction. Furthermore, these functionalized COF materials were applied to intelligent pH-responsive drug delivery and exhibited a nearly 4-fold increase in Ara-C drug release at pH=.8 than pH=7.4, which will effectively improve drug-trageting and reduce drug side effects. This study thus develops the design and synthesis of 3D stimuli-responsive COFs, and promotes the potential application of COF materials for disease theranostics.

Further detailed experimental procedures and characterization are described in the Supporting Information.

Acknowledgments

This work was supported by the National Natural Science Foundation of China (22025504, 21621001, and 21390394), ″111″ project (BP0719036 and B17020), China Postdoctoral Science Foundation (2020TQ0118 and 2020M681034) and the program for JLU Science and Technology Innovative Research Team. V.V., Q.F. and S.Q. acknowledge the collaboration in the framework of China-French joint laboratory "Zeolites".

Conflict of interest

The authors declare no conflict of interest.

Received: ((will be filled in by the editorial staff))

Published online on ((will be filled in by the editorial staff))

Reference

[1] a) A. P. Côté, A. I. Benin, N. W. Ockwig, M. O'Keeffe, A. J. Matzger, O. M. Yaghi, *Science* **2005**, *310*, 1166-1170; b) J. W. Colson, W. R. Dichtel, *Nat. Chem.* **2013**, *5*, 453-465; c) S. Y. Ding, W. Wang, *Chem. Soc. Rev.* **2013**, *42*, 548-568; d) J. L. Segura, M. J. Mancheño, F. Zamora, *Chem. Soc. Rev.* **2016**, *45*, 5635-5671; e) M. S. Lohse, T. Bein, *Adv. Funct. Mater.* **2018**, *28*, 1705553; f) Y. Yusran, X. Y. Guan, H. Li, Q. R. Fang, S. L. Qiu, *Nat. Sci. Rev.* **2020**, *7*, 170-190; g) Z. F. Wang, S. N. Zhang, Y. Chen, Z. J. Zhang, S. Q. Ma, *Chem. Soc. Rev.* **2020**, *49*, 708-735; h) X. Y. Guan, F. Q. Chen, Q. R. Fang, S. L. Qiu, *Chem. Soc. Rev.* **2020**, *49*, 1357-1384; i) K. Y. Geng, T. He, R. Y. Liu, S. Dalapati, K. T. Tan, Z. P. Li, S. S. Tao, Y. F. Gong, Q. H. Jiang, D. L. Jiang, *Chem. Rev.* **2020**, *120*, 8814-8933.

[2] a) S. S. Han, H. Furukawa, O. M. Yaghi, W. A. Goddard III, *J. Am. Chem. Soc.* **2008**, *130*, 11580-11581; b) P. Kuhn, M. Antonietti, A. Thomas, *Angew. Chem. Int. Ed.* **2008**, *47*, 3450-3453; *Angew. Chem.* **2008**, *120*, 3499-3502; c) S. Wang, Q. Y. Wang, P. P. Shao, Y. Z. Han, X. Gao, L. Ma, S. Yuan, X. J. Ma, J. W. Zhou, X. Feng, B. Wang, *J. Am. Chem. Soc.* **2017**, *139*, 4258-4261; d) H. Furukawa, O. M. Yaghi, *J. Am. Chem. Soc.* **2009**, *131*, 8875-8883; e) Y. J. Wang, Y. Z. Liu, H. Li, X. Y. Guan, M. Xue, Y. S. Yan, V. Valtchev, S. L. Qiu, Q. R. Fang, *J. Am. Chem. Soc.* **2020**, *142*, 3736-3741; f) S. S. Yuan, X. Li, J. Y. Zhu, G. Zhang, P. Van Puyvelde, B. Van der Bruggen, *Chem. Soc. Rev.* **2019**, *48*, 2665-2681;

[3] a) S. Wan, J. Guo, J. Kim, H. Ihee, D. L. Jiang, *Angew. Chem. Int. Ed.* **2008**, *47*, 8826-8830; *Angew. Chem.* **2008**, *120*, 8958-8962; b) E. L. Spitler, B. T. Koo, J. L. Novotney, J. W. Colson, F. J. Uribe-Romo, G. D. Gutierrez, P. Clancy, W. R. Dichtel, *J. Am. Chem. Soc.* **2011**, *133*, 19416-19421; c) X. S. Ding, J. Guo, X. Feng, Y. Honsho, J. D. Guo, S. Seki, P. Maitarad, A. Saeki, S. Nagase, D. L. Jiang, *Angew. Chem. Int. Ed.* **2011**, *50*, 1289-1293; *Angew. Chem.* **2011**, *123*, 1325-1329; d) G. H. V. Bertrand, V. K. Michaelis, T. C. Ong, R. G. Griffin, M. Dinca, *Proc. Natl. Acad. Sci. USA* **2013**, *110*, 4923-4928; e) M. Dogru, M. Handloser, F. Auras, T. Kunz, D. Medina, A. Hartschuh, P. Knochel, T. Bein, *Angew. Chem. Int. Ed.* **2013**, *52*, 2920-2924; *Angew. Chem.* **2013**, *125*, 2992-2996; f) Y. Du, H. Yang, J. M. Whiteley, S. Wan, Y. Jin, S. H. Lee, W. Zhang, *Angew. Chem. Int. Ed.* **2016**, *55*, 1737-1741; *Angew. Chem.* **2016**, *128*, 1769-1773; g) M. Calik, F. Auras, L. M. Salonen, K. Bader, I. Grill, M. Handloser, D. D. Medina, M. Dogru, F. Löbermann, D. Trauner, A. Hartschuh, T. Bein, *J. Am. Chem. Soc.* **2014**, *136*, 17802-17807; h) P. P. Shao, J. Li, F. Chen, L. Ma, Q. B. Li, M. X. Zhang, J. W. Zhou, A. X. Yin, X. Feng, B. Wang, *Angew. Chem. Int. Ed.* **2018**, *57*, 16501-16505; *Angew. Chem.* **2018**, *130*, 16654-16658.

[4] a) S. Y. Ding, J. Gao, Q. Wang, Y. Zhang, W. G. Song, C. Y. Su, W. Wang, *J. Am. Chem. Soc.* **2011**, *133*, 19816-19822; b) S. Lin, C. S. Diercks, Y. B. Zhang, N. Kornienko, E. M. Nichols, Y. Zhao, A. R. Paris, D. Kim, P. Yang, O. M. Yaghi, C. J. Chang, *Science* **2015**, *349*, 1208-1213; c) Q. R. Fang, S. Gu, J. Zheng, Z. B. Zhuang, S. L. Qiu, Y. S. Yan, *Angew. Chem. Int. Ed.* **2014**, *53*, 2878-2882; *Angew. Chem.* **2014**, *126*, 2922-2926; d) Y. W. Peng, Z. G. Hu, Y. J. Gao, D. Q. Yuan, Z. X. Kang, Y. H. Qian, N. Yan, D. Zhao, *ChemSusChem* **2015**, *8*, 3208-3212; e) V. S. Vyas, F. Haase, L. Stegbauer, G. Savasci, F. Podjaski, C. Ochsenfeld, B. V. Lotsch, *Nat. Commun.* **2015**, *6*, 8508; f) X. R. Wang, X. Han, J. Zhang, X. W. Wu, Y. Liu, Y. Cui, *J. Am. Chem. Soc.* **2016**, *138*, 12332-12335; g) Q. Sun, B. Aguila, J. Perman, N. Nguyen, S. Q. Ma, *J. Am. Chem. Soc.* **2016**, *138*, 15790-15796; h) H. C. Ma, C. C. Zhao, G. J. Chen, Y. B. Dong, *Nat. Commun.* **2019**, *10*, 3368.

[5] a) C. R. DeBlase, K. E. Silberstein, T. Truong, H. D. Abruña, W. R. Dichtel, *J. Am. Chem. Soc.* **2013**, *135*, 16821-16824; b) C. J. Doonan, D. J. Tranchemontagne, T. G. Glover, J. R. Hunt, O. M. Yaghi, *Nat. Chem.* **2010**, *2*, 235-238; c) T. Y. Zhou, S. Q. Xu, Q. Wen, Z. F. Pang, X. Zhao, *J. Am. Chem. Soc.* **2014**, *136*, 15885-15888; d) Q. R. Fang, Z. B. Zhuang, S. Gu, R. B. Kaspar, J. Zheng, J. H. Wang, S. L. Qiu, Y. S. Yan, *Nat. Commun.* **2014**, *5*, 4503; e) Q. Sun, B. Aguila, J. Perman, L. D. Earl, C. W. Abney, Y. Cheng, H. Wei, N. Nguyen, L. Wojtas, S. Q. Ma, *J. Am. Chem. Soc.* **2017**, *139*, 2786-2793; f) H. P. Ma, B. L. Liu, B. Li, L. M. Zhang, Y. G. Li, H. Q. Tan, H. Y. Zang, G. S. Zhu, *J. Am. Chem. Soc.* **2016**, *138*, 5897-5903; g) J. Roeser, D. Prill, M. J. Bojdys, P. Fayon, A. Trewin, A. N. Fitch, M. U. Schmidt, A. Thomas, *Nat. Chem.* **2017**, *9*, 977-982; h) X. Y. Guan, H. Li, Y. C. Ma, M. Xue, Q. R. Fang, Y. S. Yan, V. Valtchev, S. L. Qiu, *Nat. Chem.* **2019**, *11*, 587-594; i) H. Lyu, C. S. Diercks, C. H. Zhu, O. M. Yaghi, *J. Am. Chem. Soc.* **2019**, *141*, 6848-6852; j) Y. Z. Liu, Y. J. Wang, H. Li, X. Y. Guan, L. K. Zhu, M. Xue, Y. S. Yan, V. Valtchev, S. L. Qiu, Q. R. Fang, *Chem. Sci.* **2019**, *10*, 10815-10820; j) H, Wang, C. Qian, J. Liu, Y. F. Zeng, D. D. Wang, W. Q. Zhou, L. Gu, H. W. Wu, G. F. Liu, Y. L. Zhao, *J. Am. Chem. Soc.* **2020**, *142*, 4862-4871; k) Y. Yusran, H. Li, X. Y. Guan, D. H. Li, L. X. Tang, M. Xue, Z. B. Zhuang, Y. S. Yan, V. Valtchev, S. L. Qiu, Q. R. Fang, *Adv. Mater.* **2020**, *32*, 1907289; l) D. H. Li, C. Y. Li, L. J. Zhang, H. Li, L. K. Zhu, D. J. Yang, Q. R. Fang, S. L. Qiu, X. D. Yao, *J. Am. Chem. Soc.* **2020**, *142*, 8104-8108.

[6] a) H. M. El-Kaderi, J. R. Hunt, J. L. Mendoza-Cortes, A. P. Côté, R. E. Taylor, M. O'Keeffe, O. M. Yaghi, *Science* **2007**, *316*, 268-272; b) Y. B. Zhang, J. Su, H. Furukawa, Y. F. Yun, F. Gandara, A. Duong, X. D. Zou, O. M. Yaghi, *J. Am. Chem. Soc.* **2013**, *135*, 16336-16339; c) D. Beaudoin, T. Maris, J. D. Wuest, *Nat. Chem.* **2013**, *5*, 830-834; d) G. Q. Lin, H. M. Ding, D. Q. Yuan, B. S. Wang, C. Wang, *J. Am. Chem. Soc.* **2016**, *138*, 3302-3305; e) Y. Z. Liu, Y. H. Ma, Y. B. Zhao, X. X. Sun, F. Gándara, H. Furukawa, Z. Liu, H. Y. Zhu, C. H. Zhu, K. Suenaga, P. Oleynikov, A. S. Alshammari, X. Zhang, O. Terasaki, O. M. Yaghi, *Science* **2016**, *351*, 365-369; f) L. A. Baldwin, J. W. Crowe, D. A. Pyles, P. L. McGrier, *J. Am. Chem. Soc.* **2016**, *138*, 15134-15137; g) Y. X. Ma, Z. J. Li, L. Wei, S. Y. Ding, Y. B. Zhang, W. Wang, *J. Am. Chem. Soc.* **2017**, *139*, 4995-4998; h) T. Q. Ma, E. A. Kapustin, S. X. Yin, L. Liang, Z. Y. Zhou, J. Niu, L. H. Li, Y. Y. Wang, J. Su, J. Li, X. G. Wang, W. D. Wang, W. Wang, J. L. Sun, O. M. Yaghi, *Science* **2018**, *361*, 48-52; i) Y. C. Ma, Y. J. Wang, H. Li, X. Y. Guan, B. J. Li, M. Xue, Y. S. Yan, V. Valtchev, S. L. Qiu, Q. R. Fang, *Angew. Chem. Int. Ed.* **2020**, *59*, 19633-19638; *Angew. Chem.* **2020**, *132*, 19744-19749.

[7] a) H. Li, J. H. Chang, S. S. Li, X. Y. Guan, D. H. Li, C. Y. Li, L. X. Tang, M. Xue, Y. S. Yan, V. Valtchev, S. L. Qiu, Q. R. Fang, *J. Am. Chem. Soc*. **2019**, *141*, 13324-13329; b) Q. Y. Lu, Y. C. Ma, H. Li, X. Y. Guan, Y. Yusran, M. Xue, Q. R. Fang, Y. S. Yan, S. L. Qiu, V. Valtchev, *Angew. Chem. Int. Ed.* **2018**, *57*, 6042-6048; *Angew. Chem.* **2018**, *130*, 6150-6156; c) S. C. Yan, X. Y. Guan, H. Li, D. H. Li, M. Xue, Y. S. Yan, V. Valtchev, S. L. Qiu, Q. R. Fang, *J. Am. Chem. Soc*. **2019**, *141*, 2920-2924; d) Z. L. Li, H. Li, X. Y. Guan, J. J. Tang, Y. Yusran, Z. Li, M. Xue, Q. R. Fang, Y. S. Yan, V. Valtchev, S. L. Qiu, *J. Am. Chem. Soc.* **2017**, *139*, 17771–17774; e) Q. R. Fang, J. H. Wang, S. Gu, R. B. Kaspar, Z. B. Zhuang, J. Zheng, H. X. Guo, S. L. Qiu, Y. S. Yan, *J. Am. Chem. Soc.* **2015**, *137*, 8352-8355; f) H. Li, Q. Y. Pan, Y. C. Ma, X. Y. Guan, M. Xue, Q. R. Fang, Y. S.Yan, V. Valtchev, S. L. Qiu, *J. Am. Chem. Soc.* **2016**, *138*, 14783-14788; g) X. Y. Guan, Y. C. Ma, H. Li, Y. Yusran, M. Xue, Q. R. Fang, Y. S. Yan, V. Valtchev, S. L. Qiu, *J. Am. Chem. Soc*. **2018**, *140*, 4494-4498; h) H. Li, J. H. Ding, X. Y. Guan, F. Q. Chen, C. Y. Li, L. K. Zhu, M. Xue, D. Q. Yuan, V. Valtchev, Y. S. Yan, S. L. Qiu, Q. R. Fang, *J. Am. Chem. Soc*. **2020**, *142*, 13334-13338.

[8] a) X. Su, I. Aprahamian, *Chem. Soc. Rev.* **2014**, *43*, 1963-1981; b) S. M. Landge, E. Tkatchouk, D. Benítez, D. A. Lanfranchi, M. Elhabiri, W. A. Goddard, I. Aprahamian, *J. Am. Chem. Soc.* **2011**, *133*, 9812-9823.

[9] a) S. Kassem, A. T. L. Lee, D. A. Leigh, A. Markevicius, J. Solà, *Nat. Mater.* **2016**, *8*, 138–143; b) S. M. Landge, I. Aprahamian, *J. Am. Chem. Soc.* **2009**, *131*, 18269-18271; c) B. Shao, M. Baroncini, H. Qian, L. Bussotti, M. D. Donato, A. Credi, I. Aprahamian, *J. Am. Chem. Soc.* **2018**, *140*, 12323-12327; d) X. Su, S.Voskian, R. P. Hughes, I. Aprahamian, *Angew. Chem. Int. Ed*. **2013**, *52*, 10734-10739; *Angew. Chem.* **2013**, *125*, 10934-10939.

[10] a) F. J. Uribe-Romo, C. J. Doonan, H. Furukawa, K. Oisaki, O. M. Yaghi, *J. Am. Chem. Soc.* **2011,** *133*, 11478-11481; b) Z. Li, N. Huang, H. Ka, Y. Feng, S. Tao, Q Jiang, N. Yuki, I. Stephan, D. Jiang, *J. Am. Chem. Soc.* **2018**, *140*, 12374-12377; c) D. N. Bunck, W. R. Dichtel, *J. Am. Chem. Soc.* **2013,** *135*, 14952-14955; d) L. Stegbauer, K. Schwinghammer, B. V. Lotsch, *Chem. Sci*. **2014**, *5*, 2789-2793; e) X. Li, Q. Gao, J. Wang, *Nat. Commun*. **2018**, *9*, 2335.

[11] C. Bonneau, O. Delgado-Friedrichs, M. O'Keeffe, O. M. Yaghi, *Acta Crystallogr. Sect. A* **2004**, *60*, 517-520.

[12] *Materials Studio ver. 7.0*; Accelrys Inc.; San Diego, CA.

[13] A. Nagai, Z. Q. Guo, X. Feng, S. B. Jing, X. Chen, X. S. Ding, D. L. Jiang, *Nat. Commun*. **2011**, *2*, 536.

[14] a) R. Kulkarni, Y. Noda, D. K. Barange, Y. S. Kochergin, P. Lyu, B. Balcarova, P. Nachtigall, M. J. Bojdys, *Nat. Commun.* **2019**, *10*, 3228; b) D. Chen, W. Chen, G. Xing, T. Zhang, L. Chen, *Chem. Eur. J.* **2020**, *26*, 8377-8381.

[15] N. Martinez, B. Drescher, H. Riehle, C. Cullmann, H. P. Vornlocher, A. Ganser, G. Heil, A. Nordheim, J. Krauter, O. Heidenreich, *BMC Cancer* **2004**, *4*, 44.

[16] J. H. Kim, Y. S. Kim, K. Park, S. Lee, H. Y. Nam, K. H. Min, H. G. Jo, J. H. Park, K. Choi, S. Y. Jeong, R.W. Park, I. S. Kim, K. Kim, I. C. Kwon, *J. Control. Release* **2008**, *127*, 41-49.

[17] a) J. Chen, B. Zhang, F. Xia, Y. Xie, S. Jiang, R. Su, W. Wu, *Nanoscale* **2016**, *8*, 7127-7136; b) R. Ocampo-Pérez, M. Sánchez-Polo, J. Rivera-Utrilla, R. Leyva-Ramos, *Chem. Eng. J*. **2010**, *165*, 581-588; c) S. J. Sonawane, R. S. Kalhapure, T. Govender, *Eur. J. Pharm. Sci*. **2017**, *99* , 45-65.